EFFECTIVE SAR IMAGE DESPECKLING BASED ON BANDLET AND SRAD

By

Nithin Raj Rajamohanan
Supervisor : Dr. Jeffrey Zou

A thesis submitted to Western Sydney University
for the degree of Master of Research
School of Computing, Engineering and Mathematics
August 2019

WESTERN SYDNEY
UNIVERSITY

Statement of Authentication

The work presented in this thesis is, to the best of my knowledge and belief, original except as acknowledged in the text. I hereby declare that I have not submitted this material, either in full or in part, for a degree at this or any other institution.

Nithin Raj Rajamohanan

ACKNOWLEDGMENTS

This thesis is only been possible because of the support of many people to whom I would like to acknowledge for their ideas, contributions, and moral support. The research provided me opportunities to learn more about the state of the art techniques, new concepts in the related field.

Firstly, sincere gratefulness towards my supervisor Dr. Jeffrey Zou, who gave unwavering support in the completion of this thesis. I am highly indebted to the constant support, constructive and valuable suggestions during our meetings. I am also thankful for the effort he has taken in suggesting various corrections during the content writing and modifying the structure.

At last, but not least my gratitude towards my family, who was always there for support and love. I am thankful to my friends for their understanding at all times.

LIST OF PUBLICATION

- Nithin Raj Rajamohanan and Jeffrey Zou, “Effective despeckling of SAR image based on Bandlet and SRAD,” *Electronic Letters*. (submitted).

ABSTRACT

Despeckling of a SAR image without losing features of the image is a daring task as it is intrinsically affected by multiplicative noise called speckle. This thesis proposes a novel technique to efficiently despeckle SAR images. Using an SRAD filter, a Bandlet transform based filter and a Guided filter, the speckle noise in SAR images is removed without losing the features in it. Here a SAR image input is given parallel to both SRAD and Bandlet transform based filters. The SRAD filter despeckles the SAR image and the despeckled output image is used as a reference image for the guided filter. In the Bandlet transform based despeckling scheme, the input SAR image is first decomposed using the bandlet transform. Then the coefficients obtained are thresholded using a soft thresholding rule. All coefficients other than the low-frequency ones are so adjusted. The generalized cross-validation (GCV) technique is employed here to find the most favorable threshold for each subband. The bandlet transform is able to extract edges and fine features in the image because it finds the direction where the function gives maximum value and in the same direction it builds extended orthogonal vectors. Simple soft thresholding using an optimum threshold despeckles the input SAR image. The guided filter with the help of a reference image removes the remaining speckle from the bandlet transform output. In terms of numerical and visual quality, the proposed filtering scheme surpasses the available despeckling schemes.

TABLE OF CONTENTS

LIST OF FIGURES

LIST OF TABLES

1. INTRODUCTION

For more than 30 years, SAR (Synthetic Aperture Radar) images have been used commonly for remote sensing on Earth. They offer high-resolution, weather independent and day and night pictures for a variety of applications, including climate change and geoscience studies, change detection, earth system tracking and environmental, security-related applications, 2-D mapping, 3-D mapping and 4-D mapping (space and time) up to planetary exploration. SAR systems take advantage of long-range propagation features of radar signals, contemporary digital electronics, and complicated data handling capacity to provide a high-resolution image. SAR complements optical imaging techniques because the atmospheric circumstances or time of day are not restricted due to distinctive terrain reactions and cultural radar frequency objectives.

The SAR picture includes noise with distinct features that are different from general pictures acquired through standard optical sensors. Speckle noise is the sort of noise produced in SAR pictures which are triggered by mutual interference of microwave signals emitted from aircraft and has taken different paths. A distribution of Rayleigh and comparable features to multiplicative noise is observed in speckle-noise [1]. Based on aforesaid features, the picture is degraded with speckle noise and avoids transmission of the initial picture data to the observer. As a consequence, it is hard to analyze SAR pictures. It is compulsory to remove speckle noise connected with it for the countless SAR picture applications. The existence of this speckle-noise

generates a false alarm in the event of autonomous systems where SAR picture is the input. It generates enormous issues in military and other key applications. The existence of this noise creates problems in properly identifying the targets in the automatic target detection scheme. The removal of speckle noise in the SAR picture is therefore very crucial before it can be used for any of these applications. The speckle level rises as the signal's energy rises. Speckle is therefore regarded as a multiplicative noise with the value of reflectivity as its standard deviation. This makes speckle removing very hard compared to other noise seen in optical pictures.

Common areas of application of this research are SAR imaging, medical imaging, etc., where speckle noise enters when these images are acquired. With applications ranging from climate study to space exploration, SAR imaging showed its superior capabilities. The major limitation of SAR imaging is the presence of speckle noise. Computer vision-based automatic tracking using SAR is another major field of study which is limited by the presence of speckle noise. Ultrasound imaging and Optical coherence tomography are effective and highly preferred medical imaging techniques. The major drawback of these medical imaging techniques is also the presence of speckle noise interfering the image during its image capture. Preserving picture characteristics while despeckling is essential in all these instances.

Many systems are traditionally accessible for despeckling. They are widely categorized as spatial filtering, transform based filtering and nonlocal filtering schemes. Spatial filtering methods such as Lee filter [2], Kaun filter [3], Frost filter [4], etc. can efficiently remove speckle in homogeneous regions while these systems blur the image's heterogeneous regions. The 2-D wavelet transform (2DWT) [5] [6] [7] is the predominant transform domain schemes. Many other multi-scale transforms have also been created, including contourlets [8], wedgelets [9], directionlets [10],

bandlets [11] and so on. Although these filtering systems do better than the aforementioned filters, they do not provide despeckling without blurring the edge characteristics and patterns in the SAR picture.

1.1 AIM OF THE RESEARCH

Even though the existing methodologies can provide despeckling to an extent, the inefficiency to completely capture the patterns and edge features in the noisy image will limit the efficacy of these despeckling methods. Though some available schemes perform well in removing the noise, it seems to blur the heterogeneous features in the image. As heterogeneous features in the image are really important for human and computer visual analysis, removal of this useful information is a serious issue.

The primary aim of this thesis is to create an effective SAR image despeckling algorithm that can effectively preserve the heterogeneous features while despeckling the homogeneous regions.

1.2 CONTRIBUTION OF THE THESIS

The technique suggested here is the wise incorporation of three despeckling methodologies to create maximum effectiveness out of all techniques. It combines all the individual techniques to produce a better-despeckled picture visually and quantitatively.

- An adaptive picture despeckling system has been developed that can maintain the maximum significant characteristics while diluting the speckle noise.

- For a broad spectrum of noise variances, the suggested technique can be used to provide a better-despeckled image than state-of-the-art techniques.

1.3 THESIS OUTLINE

This thesis focuses on combining three despeckling schemes suitably to exploit each method and create a better despeckling scheme. The rest of the thesis is arranged as follows. In Chapter 2, various image despeckling systems are highlighted with the strength and weaknesses of each type. In Chapter 3, the main theory and implementation of the proposed methodology are explained. Experimental results and comparison of the results with state-of-the-art techniques are illustrated in Chapter 4. In Chapter 5, the entire work is summarized and a reflection is provided on the scope of further studies in the field of image despeckling.

2. LITERATURE REVIEW

SAR imaging is a significant source of data that offers high-resolution earth pictures in all circumstances of weather and lighting. It has a broad variety of applications such as land resource management, environmental protection, archaeology, disaster management, homeland security, etc., requiring various image processing operations such as target detection, classification, and image segmentation, etc. The efficiency of image processing depends strongly on the picture source quality. SAR pictures are inherently prone to speckling due to constructive and destructive interference within each resolution cell between waves returned from basic scatterers [1]. This will have a major impact on SAR image radiometric resolution and will degrade computer-aided scene analysis and human interpretation. Thus, for any SAR image processing and applications, speckle removal is a critical pre-processing phase. Owing to the launch of a big amount of radar satellites, SAR picture despeckling has been the active study subject in recent years.

In the image acquisition stage or later, the presence of speckle in SAR pictures can be decreased. Speckle reduction during image acquisition is done using multi-look processing. It is usually done by taking the means of various statistically related views of similar scenes while focusing the image in the frequency domain. [1]. The primary defect of multi-look processing technique is that it boosts radiometric resolution at the cost of spatial resolution, leading in picture smoothing.

SAR despeckling's post-image-forming methods can be divided into three wide classifications, that is, spatial filtering, transform based filtering and nonlocal filtering. In this section, these methods are described.

2.1 SAR DESPECKLING

Spatial Domain Techniques

Speckle removal of synthetic aperture radar pictures is regarded as an issue of estimation whereby the radar reflectivity estimate is performed by explicit manipulation of the speckled picture. This is equal to measuring a finite interval stochastic process. Only when the method concerned is ergodic and stationary, the assessment method will be significant. This guarantees that estimates calculated at a finite interval, approximate estimates for the entire phase. Despeckling can thus be defined as a function of the scene, non-stationary and stationary nature of the speckle, and observed signal. Usually, despeckling filters suppose speckle noise as a multiplicative wide sense stationary process with unit mean. It streamlines the processing as it is only necessary to estimate the speckle statistics once since they are continuous throughout the scene. With respect to non-stationary, stationary nature of the speckle, the despeckling filters can be categorized as Nonstationary Multiplicative Speckle Model Filters (NSMSM) and Stationary Multiplicative Speckle Model Filters (SMSM). The SMSM filters include Lee [2], Kuan [3], Frost [4] filter and MAP Gaussian filter [12] an NSMSM filter.

In a non-homomorphic manner, the SMSM filters perform the despeckling in the original domain. With a minimum mean-square error (MMSE) method linear filters are created, which work within the spatial domain. By assuming signal as gaussian, the MMSE solution develops into a linear function of the signal and noise covariance

matrix. In turn, it becomes an LMMSE (linear MMSE) filtering [13]. The strategy to LMMSE is hinged on the probability density function (pdf) of the first two moments and is really effective computationally. The SAR pictures are usually not stationary owing to the scene signal's spatial variations. These pictures are stationary locally, though. Thus it is possible to correctly estimate the first two moments relevant to put in the LMMSE strategy within a moving window. Lee [2], Kuan [3] and Frost [4] implemented the concept of adaptive filtering by implementing the LMMSE filtering locally. These conventional filters made it clear that to account for the image's non-stationarity, some kind of local adaptivity is needed. Although these filters do well in homogeneous fields to decrease the speckle, they typically display constraints in maintaining sharp characteristics and details of the initial picture owing to contour and edge losses. In order to overcome these disadvantages, contextual picture data must be considered in the despeckling algorithm. This was performed in the works reported in [14] and [15] in different respects.

The NSMSM filters, unlike SMSM speckle filters, are based on the statistical model and therefore it necessitates an understanding of a priori pdf. Easy estimation of MMSE is substituted by the advanced and assuring strategy of Bayesian a posteriori maximum (MAP). The difficult aspect of these systems is the efficient modeling of SAR image statistics. If these models are well selected, it is possible to effectively remove the noise. The suggested technique in [12] utilizes a Gaussian MAP filter and a Gamma MAP filter is used by the one suggested in [16]. The precision of the estimation of the parameter depends strongly on the quantity of information accessible. The imprecision in the estimation results in artificial biases and artifacts in the rebuilt image. A broad window will result in a precise estimation of the probability density function parameters, while a radiometric bias may be created if the amount of

independent samples is not big enough. In specific, bias relies on samples number inside the window and the autocorrelation of the texture inside the window.

Wavelet Transform Domain Techniques

The transform domain methods are primarily established using wavelet transform. It is presumed that noise here is white noise and is not dependent on the noiseless picture. For SAR despeckling, the multiplicative speckle noise must be converted into an additive nature in order to use the denoising algorithms which perform well for Additive White Gaussian Noise (AWGN). On this basis, the despeckling methods can be widely divided into two primary classifications: homomorphic and non-homomorphic.

A. Homomorphic Wavelet Approach

In a homomorphic strategy, the logarithmic transformation is applied to the data to remodel the multiplicative characteristics of the noise to an additive. One of the primary issues here is that, owing to the non-linearity of the logarithmic transform, the statistics of SAR pictures are completely altered in this phase. This requires a thorough assessment of the log-transformed speckle distribution and statistics. Many researchers have performed research over the years to describe the features of the random variables of log-transformation. Arsenault et.al [17], showed that as the number of look increases, the logarithm of speckle-noise approaches a Gaussian distribution. Thorough studies were conducted to describe the characteristics of log-transformed speckle noise and to evaluate the issues created by the log transformation of the SAR image [18]. The log-transformed speckle has been proven to be non-gaussian, particularly in the significant single-look situation, and has non-zero mean. Nevertheless, most of the homomorphic approach based despeckling systems assume

noise as a zero-mean AWGN noise. Especially for SAR pictures with elevated noise concentrations, for the purpose of radiometric conservation, mean bias issue cannot be ignored. Therefore, the biased mean must be corrected during the processing. During the denoising phase, the log transform completely shifts the dynamics of the information, resulting in unavoidable radiometric distortions.

The homomorphic method of despeckling is described in [19] use simple hard and soft thresholds. Even though the scheme uses an empirical threshold, for ordinary single-look SAR images, it is possible to provide better output than adaptive filters of the spatial domain. In addition, other works were suggested to discover a suitable range of thresholds. It includes adaptive thresholding [20], adaptive empirical shrinking [21] etc. Subsequent efficiency advancement is adept by incorporating Bayesian statistical strategy. Here to optimize the shrinkage parameter in despeckling, a priori hypothesis on the reflectivity of the scene is assumed. Many solutions based on MAP criterion were proposed and distributions like the alpha-stable distribution [22], Γ-distribution [23], Cauchy distribution [24] and normal inverse Gaussian [25] were developed for the log-transformed reflectance in the wavelet domain. As the alpha-stable distribution [22] lacks the closed-form expression, it is not possible to estimate the pdf from the noisy image and the Bayesian estimator hence developed has no closed-form. This, in turn, leads to intensive computational complexity. In [24], it proposes that there are closed-form expressions in two special cases of alpha-stable distribution, the Cauchy and the Gaussian pdfs. A straightforward Cauchy prior was suggested based on this, which has the benefit of being symmetric, with long tail and spiky peak around zero, and having only the dispersion parameter to be estimated. This leads to both MMSE and MAP Bayesian estimators being derived.

After denoising, in homomorphic strategy, the exponential procedure is carried out to convert the log-transformed pictures back to the non-logarithmic format. In the rebuild signal, a bias in the mean is introduced due to a non-zero mean in the log-transformed speckle-noise. This implies that when the logarithm is inverted after filtering, the backscatter mean is not maintained in homogeneous regions. To prevent further distortion in the restored picture, this requires to be corrected. Xie et al. [26] suggested a solution to this issue, by adding an additional processing step to adjust the mean value. Unlikely flatness after filtering due to the damping of signal difference by logarithm is another significant problem with homomorphic filtering.

B. Non-Homomorphic Wavelet Approach

Non-homomorphic technique create the denoising algorithm using the multiplicative noise model. On one hand, this gives the benefit of avoiding all the problems linked to the homomorphic strategy. On the other hand, the multiplicative model has to solve some severe modelling problems. Many non-homomorphic methods have been suggested over the years. All of these methods in different respects simplify the multiplicative noise model.

Several researchers look at the additive signal-dependent speckle model in the wavelet domain to overcome the disadvantages of the homomorphic method. When noise is independent of signal, the MMSE Wiener filtering can easily be formulated and it can perform efficiently in the wavelet domain. This is performed as a rescaling of the coefficients of the wavelet by a space-varying variable depending on the coefficients themselves SNR [27]. To derive the shrinkage factor for each wavelet coefficient, a low-complexity MMSE estimation method is suggested in [28]. In the undecimated wavelet domain, MMSE filtering was expanded to multiplicative noise

[6]. Foucher et al. [7] modeled the pdf of stationary WT wavelet coefficients using the Pearson distribution and rebuilt the despeckled picture using the MAP criterion. While this algorithm has sound performance, the Pearson distribution's elevated computational complexity makes this strategy in practice less attractive. M.Dai et al [5] provided with edge conservation an effective non-homomorphic despeckling system. F.Argenti et al [29] suggested a generalized Gaussian (GG) distribution-based despeckling system in the wavelet domain, defined by two spatially varying parameters. By the interactions between these moments and the moments of observable noisy factors, these parameters of signal-dependent noise and speckle-free reflectivity are obtained. The primary issue here is that the reflectivity pixel cross correlation is ignored to allow for a simpler estimation of GG parameters. In homogeneous fields, this hypothesis is justified, but no longer in textured fields. The same system has been expanded to resolve these problems by classifying wavelet coefficients based on their heterogeneity level [30]. Scene disparate information is very important because ergodicity and local stationarity assumptions can no longer be verified in order to obtain the statistical estimation of parameters. In addition, if the speckle is not completely formed in highly heterogeneous regions such as point objectives, it will be better to leave the area without any processing.

The significant downside of GG-based MAP alternatives, is that it can only be accomplished numerically, resulting in heavy computational costs. A Laplacian – Gussian (LG) hypothesis was used to obtain MAP estimators and minimal mean square error for the removal of speckle in ultrasound medical images [31]. It used homomorphic filtering which results in a biased estimate. Later, based on the assumption that the estimated distribution of the coefficients of the wavelet relative to the speckle-free reflectivity and the speckle noise, A MAP despeckling system was

proposed [32], approximately obeying the Laplacian and Gaussian distribution respectively. Wavelet coefficients were also classified according to their texture content, as was the case with the GG-based MAP solution. Here the computational cost in terms of the solution acquired numerically with the GG hypothesis was decreased by one order of magnitude, without substantially influencing the output in terms of the decrease of the speckle.

C. Bayesian Despeckling in the Wavelet Domain

From the point of view of signal processing, despeckling filters aim to estimate the radar reflectivity (signal of interest) based on the skewed picture (signal observed). It is possible to use Bayesian estimation methods to fix this issue. As described previously, basically MMSE or MAP equations can be used to obtain the Bayesian solution. The MMSE only needs the noise component's second order moments while the MAP needs accurate understanding of the random variables involved in the pdf.

Under the assumptions of Gaussian models, the MMSE solution becomes a linear function of signal and noise covariance matrices and is referred to as linear filtering MMSE (LMMSE). The underlying hypothesis of uncorrelated noise results in a spatial filtering of LMMSE by localizing the signal's covariance matrix. The additional hypothesis is that the local LMMSE (LLMMSE) filter will yield uncorrelated signal variants around its space-varying mean. The LMMSE solution is no longer ideal when non-Gaussianity assumptions are made on the first-order reflectivity distribution. Consequently, the LLMMSE solution is an approximation of the MMSE estimate for maximum likelihood (ML). The MMSE estimator can be expressed as a maximum posteriori(MAP) estimator in the non-Gussian situation. If the amount of looks is not too big, as described previously, SAR reflectivity is

distributed non-Gaussian. Therefore, there is a need for better estimators such as the Gamma-MAP filter where the fundamental hypothesis of Gamma-distributed texture enables a closed form MAP solution.

Directional Transform based Techniques

Since 2D WT can only provide three directional subbands in a certain resolution, SAR image despeckling with WT results in unexpected pseudo patterns in the despeckled image. Recently, despeckling systems based on various directional transformations have been implemented to resolve these problems. The DTCWT [33] [34], curvelet [35], contourlet [36], shearlet [37] and bandlet [11] [38] systems are prominent among them. Compared to those based on WT, these systems offered better outcomes. Here is a short description of these systems.

The DTCWT has the advantage of improved directional selectivity, rough shift invariance, and perfect reconstruction over the discrete transformation of the wavelet. J J Ranjani et al. suggested a DTCWT-based despeckling algorithm by considering the wavelet coefficient dependencies across distinct scales [33]. Here, in each subband, the DTCWT coefficients are simulated using a Cauchy pdf bivariate that takes into account the statistical dependence between the DTCWT coefficients. The noise-free coefficients are calculated using a MAP estimator. The transformation of Mellin from two dependent random variables is used to predict the bivariate Cauchy pdf dispersion parameter from the loud observations. The system was subsequently refined by the same researchers with a multivariate Cauchy pdf, taking into consideration the statistical dependency between the DTCWT coefficients, their neighbours and cross-scale coefficients [34].

F. Argenti et al. suggested an effective despeckling system by exploiting non-sub-sampled contourlet transformation (NSCT) multidirectional capabilities [36]. Here the noise-free NSCT coefficients are estimated based on the MAP and LMMSE criteria from the observed ones. Although this system has yielded better outcomes, owing to the non-separable filtering of NCST, the scheme's computational complexity is much greater. A non-sub-sampled shearlet transform (NSST) adaptive despeckling technique was subsequently proposed [37] in which the NSST coefficients are categorized in each subband to define the signal of concern. Here the quantitative analysis of noise variance is carried out by considering the relationship between the Laplacian pyramid and the Directional Filter Bank used in NSST. This has enhanced the scheme's spatial adaptability. Different areas were classified in SAR picture to decrease the shrinkage percentage for areas of heterogeneity while efficiently removing speckle. Compared to the earlier stated NCST-based system, this technique offered fairly excellent despeckling efficiency while well maintaining details and texture data.

Compared to wavelet, curvelet, contourlet, shearlet etc, the bandelets have adaptability. Other multi-scale geometric analysis instruments also outperform the number of its optional instructions. An edge detection and Fuzzy C Means (FCM) clustering algorithm based on Translation Invariant Bandlet Transform (TIBT) was suggested by Biao Hou et al. A comparable despeckling system with edge detection based on multi-scale Bandlet transform products was revealed later [38]. Compared to WT and other directional transform-based systems, both these systems given very good despeckling outcomes.

Non-local Despeckling Techniques

The implementation of non-local strategy has been one of the most significant developments in denoising in latest years. Non-local filtering reflects a full shift in image denoising view, since the present pixel's "real" value is no longer estimated from the pixels nearest to it, but from those pixels situated anywhere in the picture that have the most comparable background. This method is based on the observation that there are clear self-similarities in most natural pictures including SAR pictures. In pictures, most patches repeat in the picture almost the same time and again. They can be utilized to perform noise filtering once these comparable patches are recognized.

Non-local filtering mimics a real statistical average of pixels by exploiting picture self-similarity, thus enabling for powerful decrease of speckles and precise conservation of characteristics. On the downside, it needs a big amount of block-similarity measures to be calculated and is thus computationally challenging. SAR despeckling systems are described here based on a non-local strategy.

A. Probabilistic Patch-Based (PPB) Filtering

PPB may be regarded as a speckle noise NLM development [39] [40]. A similarity measure that is well adapted to SAR pictures is created here. In the context of Weighted Maximum Likelihood Estimation (WMLE), PPB is created through a more general patch-based denoising strategy. The WMLE was first introduced to the picture that Polzehl et al. denounced [41]. Contrary to this, a statistical patch-based method defines the weights in PPB. Here an appropriate patch-based weight is described to generalize the distance-based Euclidean weight used in the non-local algorithm. The distance between two patches in PPB is based on the model of the speckle distribution. This system has yielded fairly excellent outcomes in despeckling.

B. SAR Version of BM3D

The BM3D system was expanded through a non-homomorphic strategy to SAR despeckling [42]. This kind of strategy does not work well for pictures with a tiny amount of looks, since in this situation the hypothesis of Gaussian noise is not satisfied. Because the logarithmic procedure changes the dynamics of the information and consequently the distances between patches, a homomorphic method is used here. The original BM3D algorithm has been modified according to the criterion used to collect blocks in the 3D groups and the process of thresholding. In the AWGN setting the Euclidean distance-based grouping makes ideal sense because a narrower Euclidean distance corresponds to a greater probability that the two noise-free signal blocks are equivalent. However, as with SAR pictures, once the noise statistics shift, the Euclidean distance loses its meaning.

2.2 STRENGTH AND WEAKNESS OF THE DESPECKLING SCHEMES

It is not always possible to obviously assign the despeckling algorithms to one category and may sometimes belong to several classifications. The spatial domain despeckling filters perform modifications directly on the spatial pixel values, thus the computational complexity of these techniques are comparatively very less. Although these filters perform well in homogenous areas of the image, they perform very poorly in sharp characteristic regions of the image and over smooth the heterogeneous regions. In comparison to spatial domain techniques, transform domain techniques perform better despeckling both in homogenous and heterogeneous regions in the image. Transform domain technique also contains some limitations. This includes the unlikely flatness in the despeckled image while using homomorphic technique, heavy

computational cost for modelling the multiplicative speckle noise in non-homomorphic method and most importantly, the directional limitation of normal wavelet transform based technique. Directional transform resolves the directional limitations of normal transform based techniques. Non-local despeckling techniques provide better results in terms of quality. But the need of big amount of block-similarity measures to be calculated makes its computation a challenging task.

3. PROPOSED METHOD

Despeckling of SAR image is a mandatory step in every application where SAR imagery is used as the input. The multiplicative speckle noise is very hard to remove as compared to additive noises which is mostly seen in normal optical imageries. Most of the widely used techniques were explained in the previous chapter. Each technique has its own advantages and limitations. While considering a range of noise variances, it is found that the performance of each method is different. In high noise variances some despeckling filters are able to perform better, while some other filters do best in low noise variances. By in-depth study, it is possible to understand that the reason behind the limitations of each techniques and their performance variation with respect to the wide range of noises.

The proposed method is developed using combining three different despeckling schemes based on Bandlet transform, SRAD and guided filter. Each of these methods is an excellent technique in their respective categories of despeckling. The theory of each method is studied and analysed separately in this thesis.

3.1 THEORY

The SAR image which is affected with multiplicative speckle noise can be expressed as

$$i(x, y) = o(x, y) \times n(x, y) \tag{3.1}$$

where i(x,y) is the SAR image degraded by speckle, o(x,y) is the orginal image without noise and n(x,y) is the noise. x, y are pixel coordinates in x and y directions respectively.

In homomorphic despeckling methods, the log transform changes the noise model to additive, which can be easily removed by thresholding or simple averaging techniques.

The log transferred SAR image can be expressed as

$$\log(i(x, y)) = \log(o(x, y)) + \log(n(x, y)) \tag{3.2}$$

$$I(x, y) = O(x, y) + N(x, y) \tag{3.3}$$

where I (x, y) is the log transformed SAR image degraded by speckle, O (x, y) is the log transformed original image without noise and N (x, y) is the log transformed noise. After Log transformation the noise, N (x, y) is assumed as additive white noise with mean 0 and variance of σ^2 of the multiplicative noise.

In the proposed method, the log transformed SAR image is thresholded after converting into frequency domain. Here a directional transform called Bandlet transform is used to change the SAR image from spatial to frequency domain.

Bandlet transform [43] [44] is a prominent directional transform. Its adaptability based on the underlying function brings its prominence. Built on

orthogonal and biorthogonal filter banks, 2D wavelet transformation is used to obtain Bandlet transformation. Bandlet transform produces four pictures containing the input picture components of low and high frequency.

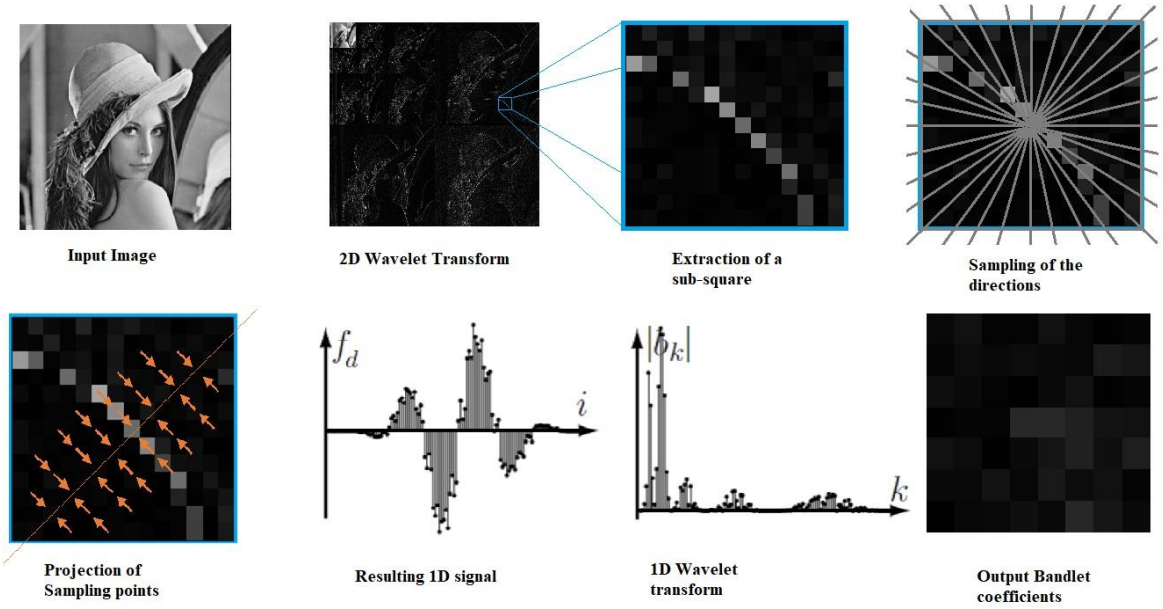

Figure 1 Overview of the Bandlet transform algorithm

The overview of Bandlet transform is given in Figure 1, A dyadic square is chosen and the input wavelet picture is constantly divided to create four fresh sub-squares in order to execute Bandlet transformation. Each sub-square is then subjected to a parameterization of the geometric flow in all feasible directions. The amount of feasible directions is about $2n^2$, where n in amount of pixels is the width of the sub-squares. The location of the sampling is projected in the possible directions. We acquire a sequence of 1D points for a specific direction d from which we can obtain the 1D discrete signal, f_d by sorting the points acquired from left to right. A 1D discrete wavelet transform is then carried out on the signal f_d. The Bandlet transform discovers the absolute best direction for a given user-defined limit T which provides

the least approximation error. The direction d minimizing the Lagrangian cost function $L(f_d)$is the best direction and gives the best geometry [62-63]. The Lagrangian cost function is expressed as,

$$L(f_d) = \| f_d - f_{dR} \|^2 + \lambda T^2 (R_G + R_B) \tag{3.4}$$

where f_{dR} is the signal retrieved from quantized coefficients obtained as a result of 1D inverse wavelet transform. R_G and R_B represent the number of bits of quantized coefficients and geometric parameter respectively. Here λ which is chosen as 3/28 is Lagrange multiplier.

After obtaining the optimum approximations in all dyadic squares, the quadtree can be constructed. By minimizing the Lagrangian cost function, the optimum approximation in the dyadic squares is acquired. The algorithm follows a bottom-up strategy in which approximations begin at the quadtree leaves i.e., the smallest dyadic squares and move up the tree with the initialization of the sub-tree cumulative Lagrangian.

The transformed coefficients are thresholded to remove the noise. Selection of threshold is a crucial part. Most of the techniques used to find the threshold, require prior knowledge about the noise, while generalized cross-validation (GCV) [45] technique doesn't require any information about the speckle noise in the SAR image to provide an optimum threshold. This technique obtains the optimal denoising threshold (τ) by discovering the threshold value that corresponds to the GCV function's minimum value.

The GCV function in the transform domain is described as a function of τ for a specific subband d as:

$$GCV_b(\tau) = \frac{\frac{1}{S_b}\left\|M_b - M_{b,\tau}\right\|^2}{\left[\frac{S_{b0}}{S_b}\right]^2} \tag{3.5}$$

where M_b is the noisy coefficients, $M_{b,\tau}$ is the noisy coefficients with the threshold applied, S_b represents number of Bandlet transform coefficients in the subband b and S_{b0} represents the number of coefficients below the threshold which were set to zero.

Bandlet based despeckling scheme is found to perform very well in low noise variances. Its performance reduces as the speckle noise increases which is mainly due to the inefficiency of Bandlet transform (BT) to find absolute best direction which provides the least approximation error. Moreover, the Bandlet transform based despeckling scheme is a homomorphic transform, where log transform is the first step in order to modify the noise model from multiplicative to additive. The remaining thresholding process are done based on the assumption that the speckle noise has approached a Gaussian distribution. But when the noise variance is very high, the log transformed speckle will be a non-Gaussian distribution with non-zero mean. This will result in unavoidable radiometric distortion in the reconstructed despeckled image.

On considering all these limitations, another non homomorphic adaptive speckle reduction technique, which works best on high noisy region is introduced. The new scheme introduced will support the bandlet based despeckling technique working parallel with it. Speckle reducing anisotropic diffusion is a best choice for it, as it does despeckling without log transforming the data and it performs well in high noisy situations.

Speckle reducing anisotropic diffusion [46] is an edge sensitive extension of conventional adaptive speckle filter. Unlike Bandlet transform based despeckling scheme, Speckle reducing anisotropic diffusion (SRAD) performs despeckling without log transforming the image. SRAD filtering is a partial differential equation (PDE) based approach to removal of speckle noise in images. The PDE-based speckle removal approach allows the generation of an image scale space without bias due to filter window size and shape. SRAD not only preserves edges but also enhances edges by inhibiting diffusion across edges and allowing diffusion on either side of the edge. Here SRAD make use of diffusion coefficient to understand the image features and suitably inhibit the speckle noise. No thresholding procedures are introduced in this method which avoid some of the deformations in the final image as in bandlet based scheme. The diffusion filter extracts and preserves the edge region while smoothing the homogeneous region to remove noise.

For an input image $I_0(x, y)$ having finite power and no zero values over the image support Ω, the output image I(x, y; t) is evolved according to a PDE given in equation (3.6) [46].

$$\begin{cases} \dfrac{\partial I(x,y;t)}{\partial t} = div\left[c(q)\nabla I(x,y;t)\right] \\ I(x,y;0) = I_0(x,y), \left(\dfrac{\partial I(x,y;t)}{\partial \vec{n}}\right)\Big|_{\partial\Omega} = 0 \end{cases} \tag{3.6}$$

where $\partial\Omega$ denotes the border of Ω, $\vec{n}$ is the outer normal to the $\partial\Omega$, and the diffusion coefficient c(q).

Diffusion coefficient c(q) as in Eq. (3.7) uses q (x, y; t) to distinguish homogeneous regions from edge regions and patterns within the image.

$$c(q) = \frac{1}{1+[q^2(x,y;t) - q_0^2(t)]/[q_0^2(t)(1+q_0^2(t))]} \tag{3.7}$$

where q (x, y; t) called an instantaneous coefficient of variation (ICOV) is expressed as Equation (3.8) and $q_0(t)$, the speckle scale function is expressed as Equation (3.9) [46].

$$q(x,y;t)=\sqrt{\frac{\left(\frac{1}{2}\right)\left(\frac{\left|\nabla I(x,y;t)\right|}{I(x,y;t)}\right)^2-\left(\frac{1}{4^2}\right)\left(\frac{\left|\nabla^2 I(x,y;t)\right|}{I(x,y;t)}\right)^2}{\left[1+\left(\frac{1}{4}\right)\left(\frac{\left|\nabla^2 I(x,y;t)\right|}{I(x,y;t)}\right)\right]^2}} \tag{3.8}$$

where I is the output image, ∇ denotes the gradient and ∇^2 is the Laplacian.

$$q_0(t)=\frac{\sqrt{\mathrm{var}[z(t)]}}{\overline{z(t)}} \tag{3.9}$$

where $\mathrm{var}[z(t)]$ and $\overline{z(t)}$ are the intensity variance and mean over a homogeneous region at t, respectively.

The instantaneous coefficient of variation function, q (x, y; t) represents high values in the edge regions, or high-contrast features and low values in homogeneous regions. It was determined that the diffusion coefficient plays a role in detecting the edge regions in an image with speckle noise. The function c(q) removes the noise or preserves the edges through smoothing applied according to the region of the image.

In cases where the values of q (x, y; t) and the speckle scale function $q_0(t)$ are approximately the same, c(q) detects the image as a homogeneous region and smoothing is performed to remove noise. On the other hand, in cases where the value of q (x, y; t) is larger than the value of $q_0(t)$, c(q) is considered an edge region and thus the edge region is preserved by not performing smoothing.

Therefore q(x, y; t) and $q_0(t)$ are adjusted according to the region of the input image in order to remove the speckle noise and preserve the edge. In addition, SRAD processes the data directly to preserve the useful information in the image, unlike conventional methods used for processing log-compressed data.

SRAD performs well in high noise variance and the performance reduces slightly as the noise variance decrease. In very low noise variance, SRAD is showing over smoothing of fine patterns and edges in the image causing it reduce its performance.

Usually in most of the fusion despeckling techniques, SRAD is mainly considered as the pre-processing step. This serial arrangement might cause to lose some important feature in the input image which will be hard to regain. While in the proposed method we use SRAD parallel to Bandlet transform based despeckling scheme. It is organised in this way in order to utilise all the advantages of both the techniques. Here the limitation of any of the two despeckling schemes is not limiting the other one's performance. This innovative way of arrangement helps to completely exploit all the best features of both the techniques.

In the final stage of proposed method, the outputs from both the techniques are used as an input to a guided filter. The guided filter uses SRAD despeckled image as guided image to further despeckle the bandlet based despeckled image, which in turn produces an outstanding despeckled image compared to all other techniques individually for all noise variance in a wide range. The ability of filter to provide good edge preserving smoothing property along with the ability to provide better structured output makes its suitable for the final stage of proposed despeckling scheme.

A guided filter is one that removes noise while preserving input image information by using a guidance image [47]. The guidance image is a reference image

used to reduce noise [47]. The key assumption of the guided filter is that the guidance, I, and the filtering output, g, are expressed in Equation (3.10) as a local linear model:

$$g_i = a_k I_i + b_k \forall i \in \omega_k \tag{3.10}$$

where a_k and b_k are constants in a window ω_k, and g_i is the output image. To determine the linear coefficients (a_k , b_k) defined in Equation (3.10), the output image g_i , is defined as shown in Equation (3.11).

$$g_i = p_i - n_i \tag{3.11}$$

where p_i and n_i denote the input image and the image noise, respectively. The linear coefficients are obtained via Equation (3.12), which minimizes the difference between the input image and the output image.

$$E(a_k, b_k) = \sum_{i \in \omega_k} ((a_k I_i + b_k - p_i)^2 + \in a_k{}^2) \tag{3.12}$$

where $\in$ is a normalization parameter that prevents a_k from becoming infinitely large. The solution minimizing Equation (3.13) can be obtained via linear regression as follows.

$$\begin{aligned} a_k &= \frac{\frac{1}{|\omega|}\sum_{i \in \omega_k}(I_i p_i - \mu_k \bar{p}_k)}{\sigma_k^2 + \in} \\ b_k &= \bar{p}_k - a_k \mu_k \end{aligned} \tag{3.13}$$

where μ_k and σ_k^2 are the mean and variance of the guide image, respectively, in the region ω_k, and $|\omega|$ is the number of pixels in a window, ω_k . $\bar{p}_k = \frac{1}{|\omega|}\sum_{i \in \omega_k} p_i$ is the average of p in ω_k . By obtaining the linear coefficients (a_k , b_k), the filter output, g_i , according to Equation (3.10) can be obtained. However, since pixel, i, has several overlapping ω_k , g_i is not identical. However, this can be mitigated by averaging all

possible values of g_i via a simple method. After computing (a_k , b_k) for all windows, ω_k , g_i can be obtained as follows:

$$g_i = \frac{1}{|\omega|} \sum_{k|i \in \omega_k} (a_k I_i + b_k) \tag{3.14}$$

where the output from the SRAD, I(x,y) evolves according to the partial differential equation (PDE) is used as the I_i in guided filter to further despeckle the input image p_i , which is obtained from Bandlet based scheme.

3.2 IMPLEMENTATION

The proposed scheme is an efficient organisation of three different, efficient despeckling techniques. It works in a hand by hand manner to achieve an output which performs better than state of the art techniques available. These individual techniques are the best schemes in their categories of despeckling methods. Though they perform best among a particular range of noises, for a wide range of SAR images with different noise variances, they may fail to provide best result at all time. This drawback of the individual techniques is wisely removed using organising them in a perfect manner and allowing them to work side by side, without limiting their individual capabilities. The implementation is performed after careful analysis of each sections individually.

Implementation of the proposed scheme is explained below.

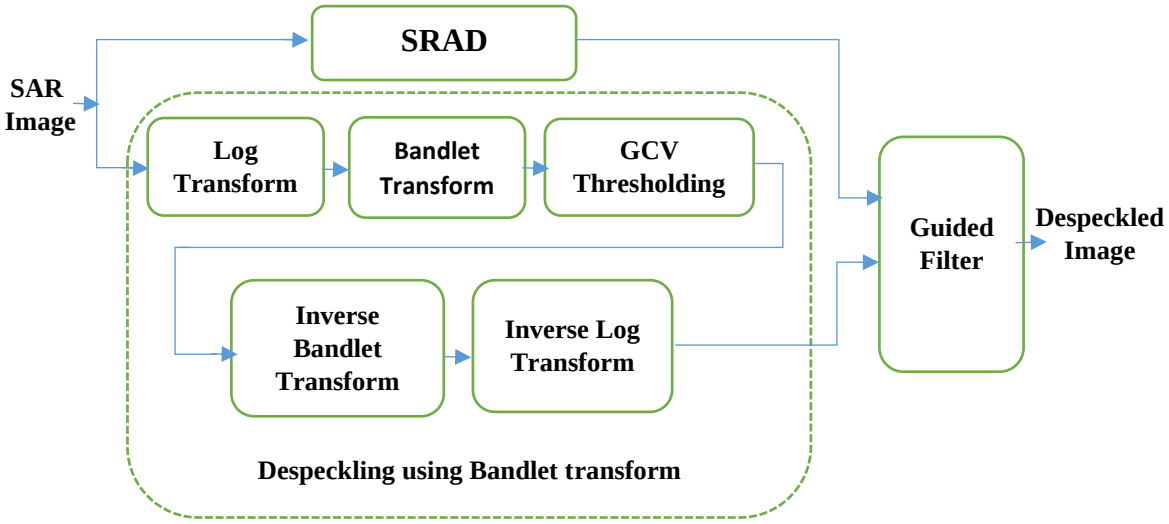

Figure 2 Block diagram of the proposed algorithm

The block diagram for the proposed algorithm is given in Figure 2. Here the SAR image suffering from multiplicative speckle noise is applied to both SRAD and Bandlet based scheme parallel.

Bandlet transform here is used in homomorphic method. The bandlet based scheme first log transform the SAR image. This will model the speckle noise to additive from multiplicative. Then Bandlet transform is performed on the log transformed image to decompose the image to Bandlet coefficient. The main feature of bandlet transform which helps in despeckling is that it distributes the noise energy over all the coefficients while the significant image features are concentrated in a few Bandlet coefficients. As a result, the influence of noise on the large signal coefficients will be small.

The bandlet coefficient then obtained is then soft threshold to remove the noise content from the coefficient. The precise selection of threshold value is very important as a lower threshold can leave behind noise and higher threshold can remove important high frequency features of the image. The optimum threshold is found here by using

Generalised Cross Validation (GCV) technique proposed by Jansen et al [57]. The main advantage of GCV technique is that it can be used to estimate the optimal threshold without having the knowledge of the noise variance. The thresholded coefficients are then used to create despeckled image using inverse Bandlet transform. In order to compensate for the log-transform, an exponential transform is applied the despeckled image to bring it to the original form.

The SRAD filter on the other hand does not utilise thresholding technique in homomorphic method. It uses diffusion coefficient to distinguish the homogenous regions from edge regions in the image. Since SRAD process the data directly, it preserves some useful information which transform domain filtering lacks due to log-transform. In the case of high noise variances, the Bandlet transform fails to find the optimum directions in the sub-image causing its poor performance. In such cases the Guided filter which performs better, helps to retain the important features Bandlet transform fails to provide.

The output from the SRAD is given as one of the input to a Guided filter which is the last stage of the proposed filter. The SRAD output serves us the reference image to further despeckle the output of Bandlet based despeckling scheme. As the guided filter has the ability to edge preserve smoothing and to provide more structured output, the extra information from SRAD filter helps to produce a better image than the bandlet based scheme.

Due to this efficient and wise organization of blocks, it is possible to combine the effectiveness of each block constructively. By combining both SRAD and Bandlet based despeckling techniques, with Guided filter, it is possible to provide a best despeckling method for despeckling of a range of SAR images.

The proposed scheme involves five major steps which are given below.

Step 1: SRAD despeckling

Step 2: Bandlet decomposition

2.1 On input SAR image, logarithmic transformation is performed.

2.2 Three level of Bandlet transform (BT) is computed.

Step 3: Threshold computation.

3.1 For all subbands,except low frequency subband, compute the GCV threshold.

3.2 Noise-free coefficients are obtained after using soft thresholding rule with computed GCV threshold on BT coefficients.

Step 4: Image reconstruction

4.1 Using inverse BT, from threshold applied noise-free coefficients image is reconstructed.

4.2 On the reconstructed image, perform inverse logarithmic transformation.

Step 5: Final Processing

5.1 Output from SRAD is given as reference image to Guided filter.

5.2 Despeckle the output of Bandlet based scheme using Guided filter.

4. EXPERIMENT RESULTS AND COMPARISONS

The performance of the proposed scheme is verified on both the synthetic and real SAR images. The synthetic SAR image is generated from standard benchmark noise-free images added with speckle noise. Here an amplitude speckled Lena image of size 512 x 512, disturbed with fully developed speckle with noise variance 0.01 is taken for experiments. These images exhibited the characteristics of multiplicative noise following Rayleigh distribution.

To evaluate the performance of the image despeckling technique, the peak signal-to-noise ratio (PSNR) is used. All image processing was performed using MATLAB R2016a.

In the proposed method, three levels of two dimensional decomposition using Biorthogonal (bior-6.8) wavelet were carried out. Biorthogonal wavelet gives better results as compared with Haar wavelet as it effectively smooths out the noise in flat regions due to the good support of its scaling function. Also the property of linear phase makes Biorthogonal wavelet ideal for image reconstruction. The proposed algorithm is compared with state of the art filtering techniques, such as SRAD, Wavelet Transform based despeckling and Bandlet transform based despeckling algorithm to evaluate the speckle noise reduction performance.

For Synthetic SAR image, the improvement in performance was evaluated in terms of peak signal-to-noise ratio (PSNR). The PSNR comparison of Synthetic Lena image is given in Table 1, with best results in bold.

Table 1 PSNR values of synthetic Lena SAR image for different despeckling schemes.

Despeckling Scheme	**PSNR (dB)**
Synthetic SAR image	25.6575
SRAD filtering **[46]**	24.8676
Wavelet Despeckling **[28]**	28.3531
Bandlet Despeckling **[11]**	28.4557
Proposed Method	**31.6890**

The visual quality is also used to evaluate the performance of the proposed scheme. Denoising in smooth regions can be achieved by most of the algorithms, but high visual quality is due to the preservation of image edges and textures which makes the difference. Figure 3 presents the comparison of the despeckled Lena image corrupted with speckle noise. Figures 3(a) and (b) are noise-free Lena image and its speckled versions respectively. Figures 3(c), (d), (e) and (f) shows the despeckled Lena images obtained by SRAD, Wavelet based despeckling scheme, Bandlet based despeckling scheme and the proposed scheme respectively. The visual quality of the despeckled image using the proposed scheme is evidently better because of sharper edges and texture.

Figure 3 Synthetic Lena SAR image despeckling results.

(a) Original noise free image. (b) Noisy image. (c) Despeckled image using SRAD. (d) Despeckled image using Wavelet Transform. (e) Despeckled image using Bandlet transform (f) Despeckled image using proposed scheme.

The proposed method was repeated with wide range of noise variances and it was found that at lower noise variances, Bandlet transform perform better than other methods and as the noise variance increases the performance of Bandlet transform decreases. This is mainly due to the inability of transform to find the features in the image in high noise variances and the noise characteristics deviates from the Gaussian white noise assumption during the homomorphic transformation. While SRAD performs better in high noise variance and seems to lower the performance in low noise variance as it over smooth important features in the image. The proposed method make use of features of both the techniques and combined using guided filter to outperform rest of the despeckling methods. Figure 4 shows PSNR values obtained using SRAD, Wavelet, Bandlet and the proposed schemes for a range of noise variances. It can be seen from this figure that the proposed scheme shows huge improvement from the rest of the despeckling methods for all noise levels.

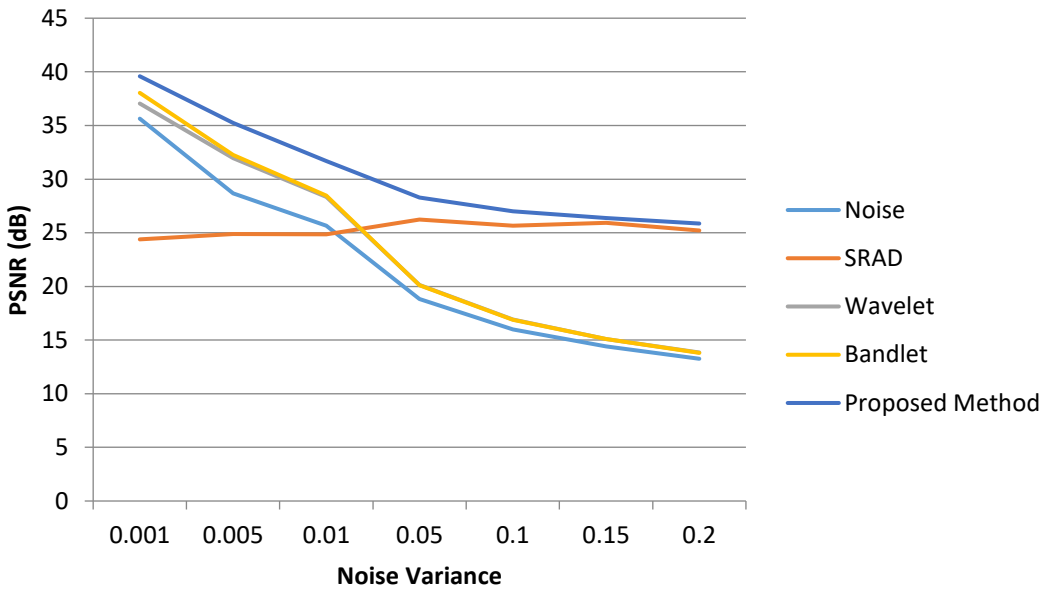

Figure 4 Relation of PSNR with noise variance for synthetic Lena SAR.

Proposed methodology has been tested with actual SAR images also. Since the noiseless image is not available for real SAR image, evaluation of despeckling capability cannot be assessed by using PSNR. Two different evaluation matrices will be used to assess the quality of despeckled SAR image. For the evaluation of capability of despeckling over a homogeneous area in an image, Equivalent Number of Looks (ENL) is used as the performance parameter.

Equivalent Number of Looks (ENL) is defined as:

$$ENL = I\left(\frac{\mu^2}{\sigma^2}\right) \qquad (4.1)$$

where $I = \begin{cases} 1 & \text{for intensity format SAR images} \\ \frac{4}{\pi} - 1 & \text{for amplitude format SAR images} \end{cases}$

and μ and σ^2 are the mean and variance values respectively over the homogeneous area.

Since the mean value represents a SAR image's average brightness, image calibration must be maintained. Image variance refers to the range at which the picture pixels deviate from the mean. A reduced variance provides a smoother, cleaner picture. The denounced picture should therefore maintain the picture mean and reduce its variance. Better despeckling corresponds to a big ENL value, With the perfect filtering infinity. In a homogeneous region, the radiometric conservation can also be evaluated by comparing the value in the initial and filtered pictures of the local mean backscattering reflectivity. A successful speckle reduction filter should not change a homogeneous region's mean intensity considerably.

A good despeckling scheme not only smooth the homogenous regions but also will be able to preserve the edges and patterns, the high frequency features, in the image. For the evaluation capability of edge preservation in the despeckled image, Edge Save Index (ESI) is used as the performance parameter.

$$ESI\_H = \frac{\sum_{x=1}^{m}\sum_{y=1}^{n-1}\left|F_{x,y+1} - F_{x,y}\right|}{\sum_{x=1}^{m}\sum_{y=1}^{n-1}\left|O_{x,y+1} - O_{x,y}\right|} \tag{4.2}$$

$$ESI\_V = \frac{\sum_{y=1}^{n}\sum_{x=1}^{m-1}\left|F_{x+1,y} - F_{x,y}\right|}{\sum_{y=1}^{n}\sum_{x=1}^{m-1}\left|O_{x+1,y} - O_{x,y}\right|} \tag{4.3}$$

where O is the original noisy image, F is the reconstructed image, m is the row number and n is the column number of the image.

ESI_V and ESI_H gives the edge preservation capability in vertical direction and horizontal direction of the despeckling scheme respectively. As ESI value increases the edge save ability of the scheme also increases.

Thus for a better despeckling scheme the ENL value for the homogenous region inside the image should be higher and ESI for the whole image should be closer to 1.

Real SAR images in amplitude and intensity formats have been used for evaluation. Figures 5–7 show the visual comparison of the despeckled versions of these images obtained by SRAD filtering, wavelet based despeckling method, bandlet based despeckling method and proposed despeckling method. Two homogeneous regions in these images are used to compute the ENL. These areas are highlighted in the noisy SAR images. The ENL and ESI values obtained are listed in Tables 2–4.

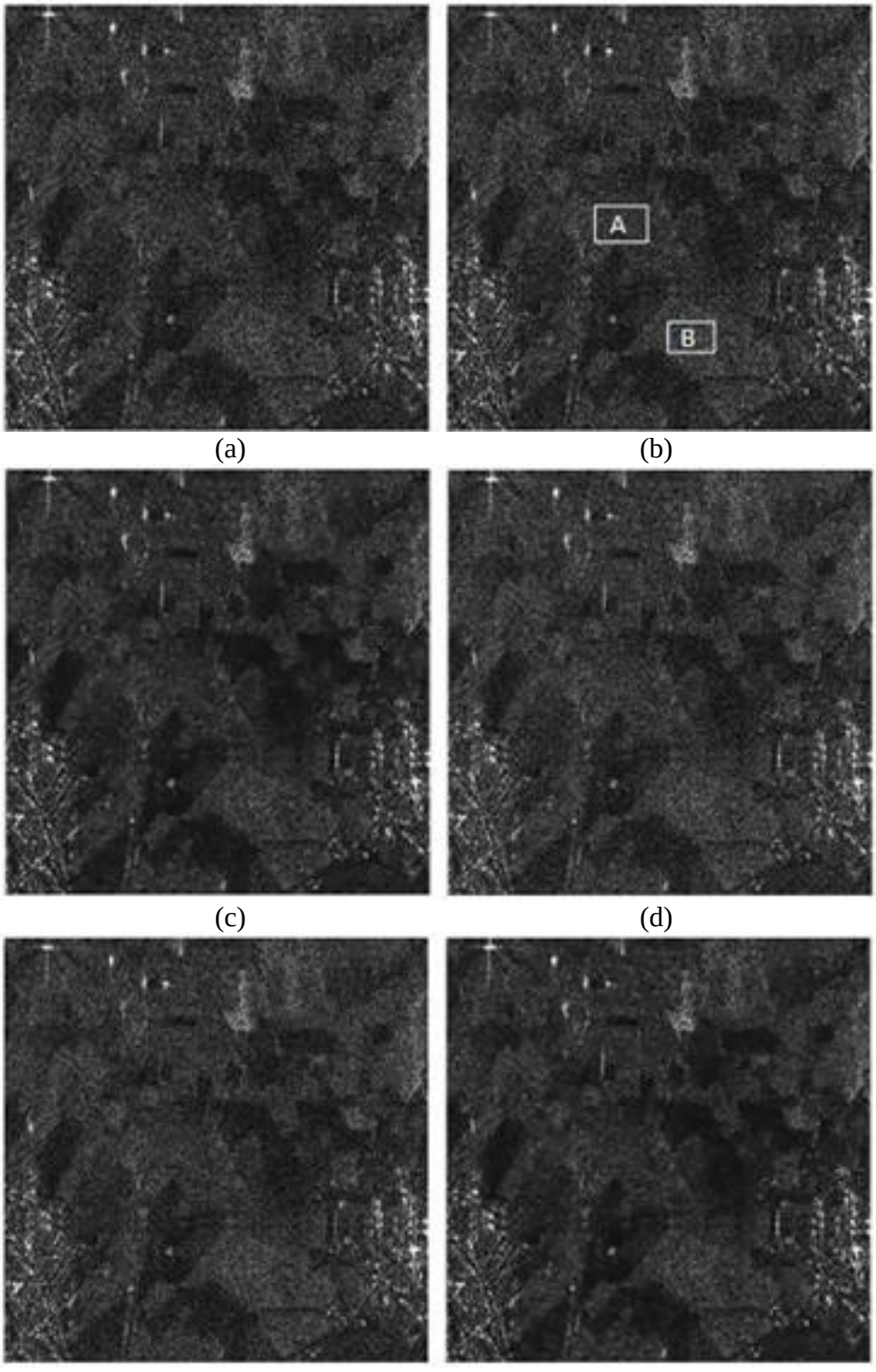

Figure 5 Sentinel-1 SAR image despeckling results.

(a) Original SAR image. (b) Image showing regions A and B. (c) Despeckled image using SRAD. (d) Despeckled image using Wavelet Transform. (e) Despeckled image using Bandlet transform (f) Despeckled image using proposed scheme.

Figure 5 shows the despeckling results of Sentinel-1 SAR image. Original SAR image and Image showing selected two homogenous regions A and B for the calculation of ENL is shown in Figures 4(a) and 4(b). Despeckled image using SRAD, Wavelet transform and Bandlet transform is shown in Figures 4(c), 4(d) and 4(e). Despeckled image using proposed scheme is shown in Figure 4(f).

Using visual inspection of the image, it can be seen that the proposed image shows better despeckling in the homogenous regions and better structural information than in SRAD filtering output. Quality of despeckling can be assessed by the qualitative analysis of ENL and ESI values of the despeckled output. Table 2 shows the ENL and ESI values for the Sentinel-1 SAR image of the despeckling scheme along with the proposed despeckling scheme.

Table 2 ENL and ESI values of Sentinel-1 SAR image with different despeckling schemes applied.

	ESI_H	**ESI_V**	**ENL_A**	**ENL_B**
Noise	1	1	13.5355	12.7078
SRAD **[46]**	0.597	0.5813	28.7282	18.6363
Wavelet **[28]**	0.877	0.8722	17.3103	16.2607
Bandlet **[11]**	**0.8846**	**0.8789**	17.3985	16.2712
Proposed Method	0.8344	0.8289	**32.504**	**20.345**

It is observed that the proposed scheme provides a substantial improvement in ESI_H and ESI_V values than SRAD and a slight lower value than wavelet and bandlet based scheme. Even though the ESI value is slightly lower, the considerable

improvement in the ENL values in both the regions over the other compared methods shows the effectiveness of the proposed despeckling scheme. Here due to high ENL values the proposed despeckling scheme is able to effectively suppress the speckle noise in homogenous regions while saving comparable feature information in the image. Thus even while removing a good amount of noise, proposed method preserves edges and details well and thereby providing better visual quality.

For the verification of the improvement of despeckling of the proposed method in real SAR image, the scheme is applied on TerraSAR-X spotlight SAR image (Figure 6) and TerraSAR-X StripMap SAR image (Figure 7). Despeckled images of proposed method along with SRAD, Wavelet and Bandlet based scheme are shown in Figure 6 and Figure 7.

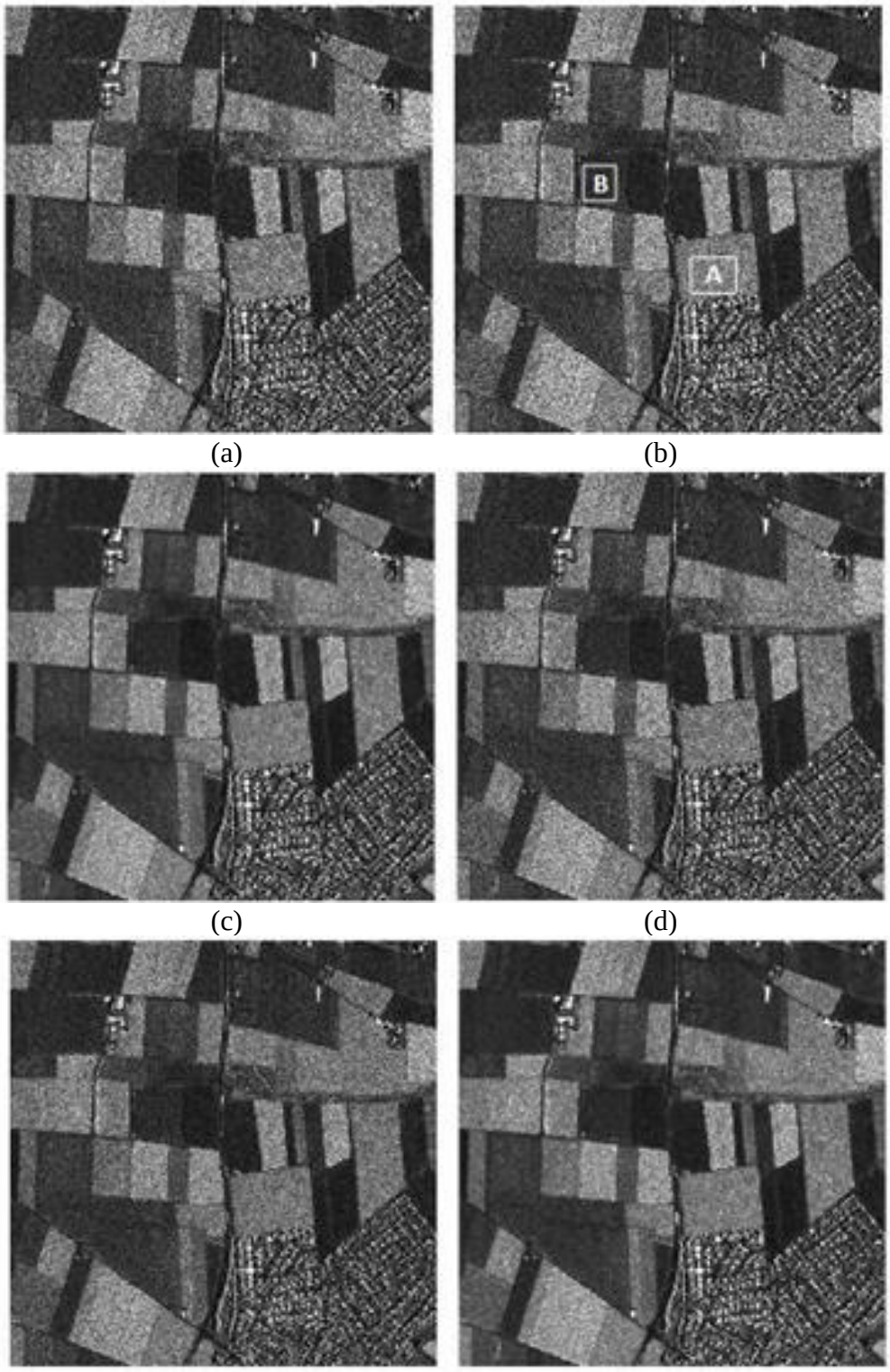

Figure 6 TerraSAR-X spotlight image of Noerdlinger Ries Despeckling results.

(a) Original SAR image. (b) Image showing regions A and B. (c) Despeckled image using SRAD. (d) Despeckled image using Wavelet Transform. (e) Despeckled image using Bandlet transform (f) Despeckled image using proposed scheme.

Improvement in despeckling of the proposed scheme is visible in the visual examination of the despeckled outputs. It is evident that there is reduced speckle content compared to wavelet and bandlet outputs. In comparison to SRAD the proposed scheme gives better details and feature preservation. Qualitative analysis of the despeckling scheme for the TerraSAR-X spotlight image is given in Table 3.

Table 3 ENL and ESI values of TerraSAR-X spotlight image with different despeckling schemes applied.

	ESI_H	**ESI_V**	**ENL_A**	**ENL_B**
Noise	1	1	17.8187	17.8333
SRAD **[46]**	0.5095	0.4984	46.0461	81.3943
Wavelet **[28]**	0.8631	0.859	24.0484	24.1522
Bandlet **[11]**	**0.8721**	**0.8682**	24.5861	24.9557
Proposed Method	0.8508	0.8497	**47.465**	**91.2074**

Here ESI_H and ESI_V of proposed scheme shows comparable feature saving capability with respect to Wavelet and Bandlet transform. In terms of speckle suppression proposed method provide high ENL value compared to all other methods. This confirms the elite performance of proposed methodology compared to the state of the art despeckling techniques.

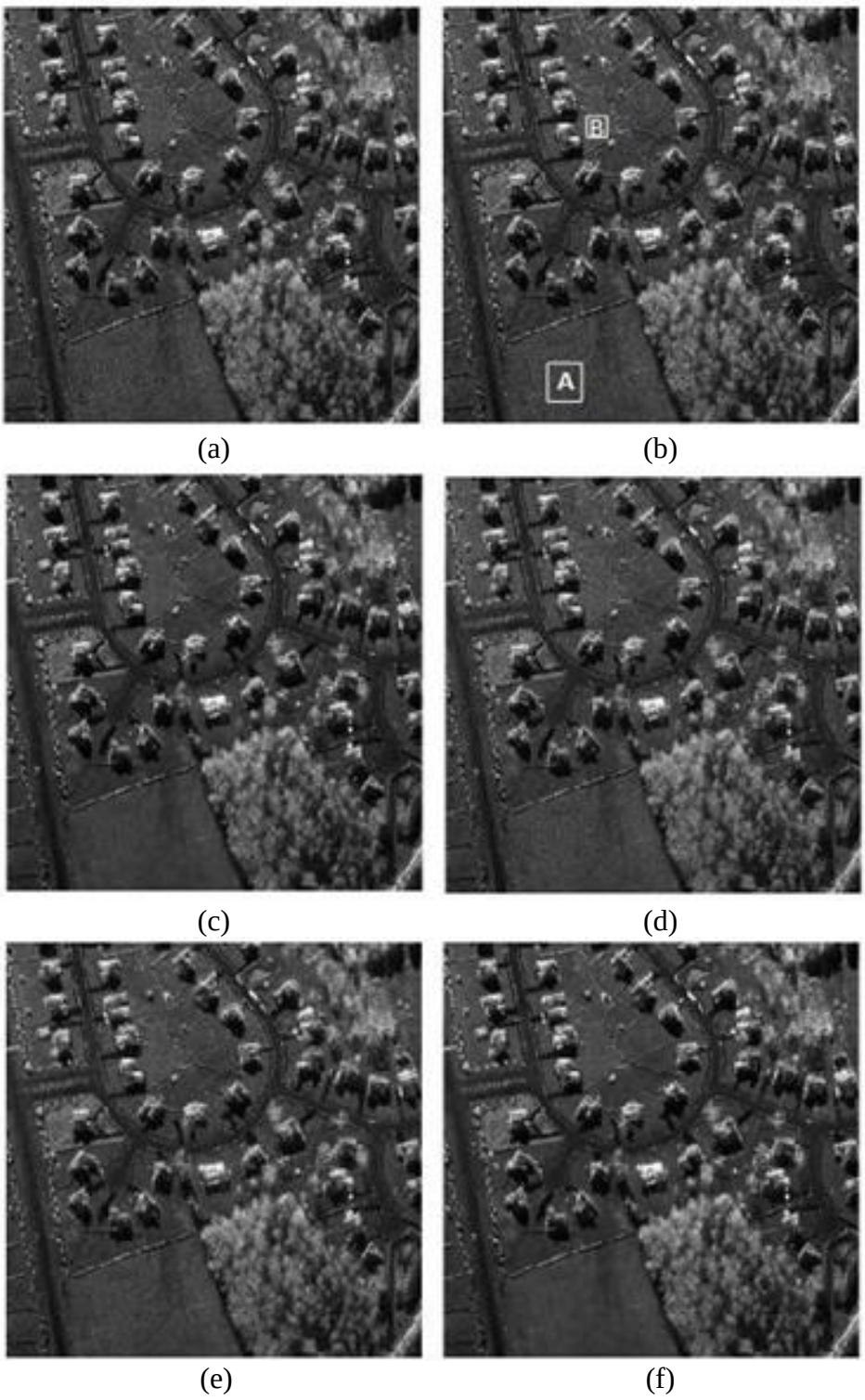

Figure 7 TerraSAR-X StripMap SAR image despeckling results.

(a) Original SAR image. (b) Image showing regions A and B. (c) Despeckled image using SRAD. (d) Despeckled image using Wavelet Transform. (e) Despeckled image using Bandlet transform (f) Despeckled image using proposed scheme.

Visual analysis of the despeckling scheme is done on TerraSAR-X StripMap SAR image also. It shows improved despeckling by the proposed method compared to other despeckling techniques. For detailed visual analysis of Despeckling results of TerraSAR-X StripMap SAR image, Figure 8 provides zoomed version of despeckling results. Improvement in the proposed method can be clealy seen here.

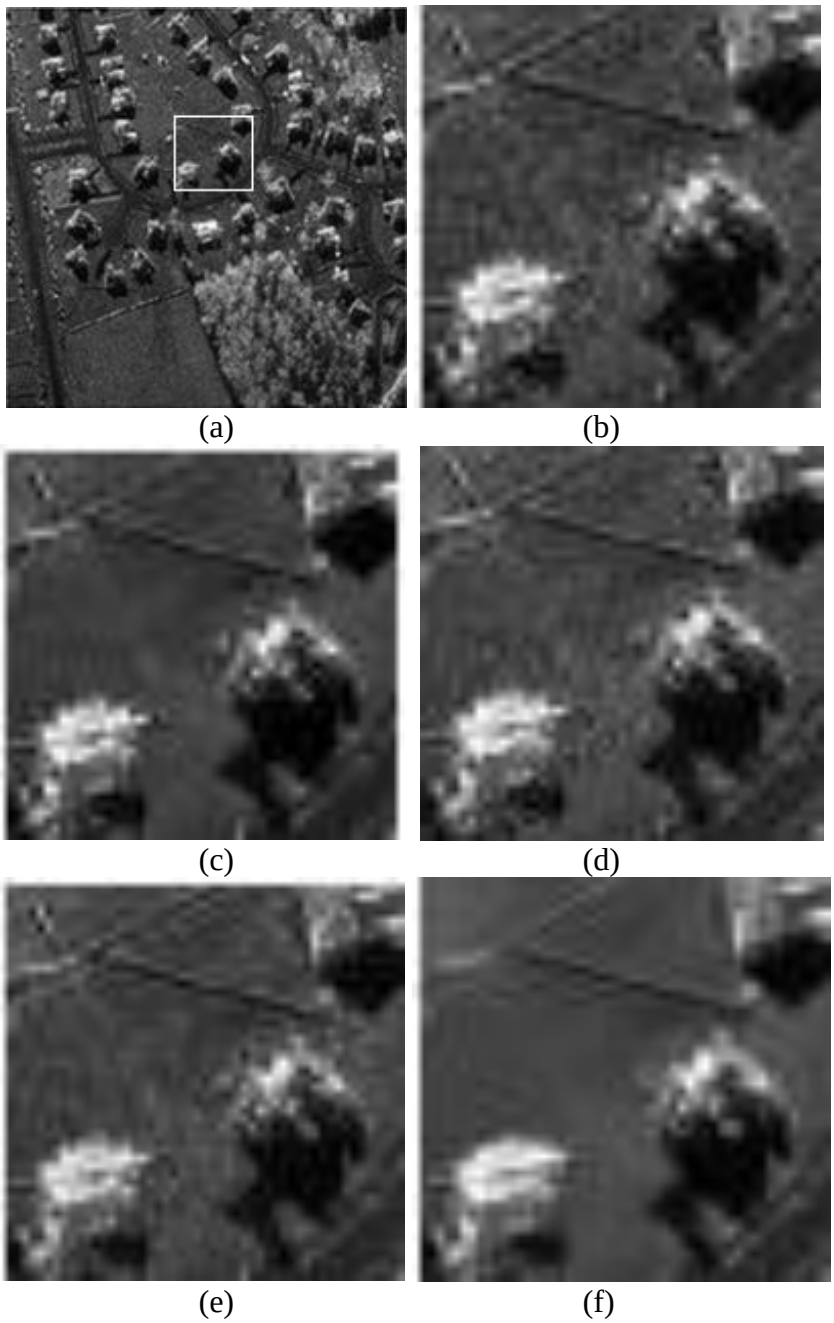

Figure 8 Zoomed TerraSAR-X StripMap SAR image despeckling results.

(a) Original SAR image with zoomed area highlighted . (b) Zoomed section of orginal SAR image. (c) SRAD. (d) Wavelet Transform. (e) Bandlet transform (f) Proposed scheme.

Table 4 shows the quantitative analysis for TerraSAR X StripMap SAR image. Both ENL and ESI metrics are tabulated for the proposed method and state of the art despeckling techniques.

Table 4 ENL and ESI values of TerraSAR-X StripMap SAR image with different despeckling schemes applied.

	ESI_H	**ESI_V**	**ENL_A**	**ENL_B**
Noise	1	1	51.7836	63.8104
SRAD **[46]**	0.7288	0.728	262.3645	238.4348
Wavelet **[28]**	0.8511	0.8477	87.5875	112.1122
Bandlet **[11]**	**0.8602**	**0.8566**	87.6842	112.8751
Proposed Method	0.8545	0.8501	**274.9461**	**248.8645**

Here also for high ESI values, the proposed methodology can provide better ENL values in both the two regions.This shows the improvement in the proposed deapeckling scheme.

5. CONCLUSION

A novel SAR image despeckling scheme proposed combines SRAD filtering, Bandlet based despeckling scheme and Guided filter. These techniques are combined in an efficient way to provide a better despeckled image. Both the quantitative and the visual analysis shows the proposed scheme outperforms the state of the art despeckling schemes. It is also observed that the proposed scheme is able to provide better despeckled outputs for a range of noise variances. The scope of the research is still open for optimization in terms of speed. The extension of the scheme to colour and video SAR despeckling will find more potential applications. The future works are aimed for addressing these problems.

REFERENCES

[1] M. Afonso and J. Sanches, “Image reconstruction under multiplicative speckle noise using total variation.,” *Neurocomputing,* vol. vol.150., pp. 200-213., Feb.2015..

[2] J. Lee, “Digital image enhancement and noise filtering by use of local statistics.,” *IEEE Trans.Pattern Anal,Mach.Intell.,* vol. 2, no. 2, pp. 165-168., 1980.

[3] D. Kuan, A. Sawchuk, T. Strand and P. Chavel, “Adaptive noise smoothing filter for images with signal- dependent noise.,” *IEEE Trans. pattern Anal. Mach. Intell.,* vol. 7, no. 2, pp. 165-177., 1985..

[4] V. Frost, J. Stiles, K. Shanmugan and J. Holtzman, “A model for radar images and its application to adaptive digital filtering of multiplicative noise.,” *IEEE Trans. Pattern. Anal. Mach. Intell.,* vol. 4, no. 2, pp. 157-166, 1982..

[5] M. Dai, C. Peng, A. K. Chan and D. Loguinov, “Bayesian wavelet shrinkage with edge detection for SAR image despeckling,” *IEEE Trans.Geosci.Remote Sens.,* vol. 42, no. 8, pp. 1642-1648, Aug.2004.

[6] F. Argenti and L. Alparone, “Speckle removal from SAR images in the undecimated wavelet domain.,” *IEEE Trans.Geosci.Remote Sens.,* vol. 40, no. 11, pp. 2363-2374., 2002.

[7] S. Foucher, G. B. Benie and J. M. Boucher, “Multiscale MAP filtering of SAR images,” *IEEE Trans. image processing,* vol. 10, pp. 49-60, Jan.2001.

[8] M. Do and M. Vetterli, “The contourlet transform:an efficient directional multi resolution image representation.,” *IEEE Trans.Image Process.,* vol. 14, no. 12, pp. 2091-2106, 2005.

[9] D. Donoho, “Wedgelets: nearly minimax estimationof edges.,” *Ann Statist.,* vol. 27, pp. 859-897, 1999.

[10] R. Sethunadh and T. Thomas, “SAR image despeckling using adaptive multi-scale products thresholding in directionletdomain,” *Electron Lett.,* vol. 49, no. 18, pp. 1183-1184, 2013.

[11] N. Raj, R. Sethunadh and P. R. Aparna, “Object detection in SAR image based on bandlet transform,” *J.Vis. Commun.Image R.,* vol. 40, pp. 376-383, 2016.

[12] A. Lopes, E. Nezry, R. Touzi and H. Laur, “Maximum a Posteriori speckle filtering and first order texture models in SAR images,” *in Proc. IGARSS,Washington,DC,* vol. 3, pp. 2409-2412, May 1990.

[13] S. Parrilli, M. Poderico, C. Angelino and L. Verdoliva, “A nonlocal SAR image denoising algorithm based on LLMMSE wavelet shrinkage,” *IEEE Transactions on Geoscience and Remote sensing,* vol. PP, pp. 1-11, 2011.

[14] G. Lee, “Refined filtering of image noise using local statistics,” *Comput.Graph. Image process,* vol. 15, p. 4, 1981.

[15] A. Lopes, R. Touzi and E. Nezry, “Adaptive speckle filters and sceneheterogeneity,” *IEEE Trans.Geosci.Remote sens.,* vol. 28, no. 6, pp. 992-1000, 1990.

[16] A. Baraldi and F. Parmigiani, “A refined Gamma MAP SAR specklefilter with improved geometrical adaptivity,” *IEEE Trans. On Geosci.and Remote Sensing,* vol. 33, pp. 1245-1257, Sept. 1995.

[17] H. Arsenault, G. April and H. H. Arsenault, “Properties of speckle integrated with a finite aperture and logarithmically transformed,” *J.Opt.Soc.Am.,* vol. 66, no. 11, pp. 1160-1163, 1976.

[18] H. Xie, L. Pierce and F. Ulaby, “Statstical properties of logarithmically transformed speckle,” *IEEE Transactions on Geoscience and Remote Sensing,* vol. 40, no. 3, pp. 721-727, Mar.2002.

[19] L. Gagnon and A. Jouan, “Speckle filtering of SAR images - A comparative study between complex-wavelet based and standard filters.,” *Proc.SPIE.,* vol. 3169, pp. 80-91, 1997.

[20] J. Sveinsson and J. Benediktsson, “Almost translation invariant wavelet transformations for speckle reduction of SAR images.,” *IEEE Transactions on Geoscience and Remote Sensing.,* vol. 41, no. 10, pp. 2404-2408, Oct.2003.

[21] S. Fukuda and H. Hirosawa, “Smoothing effect of wavelet-based speckle filtering: the Haar basis case.,” *IEEE Transactions on Geoscience and Remote sensing.,* vol. 37, pp. 1168-1172, Mar.1999.

[22] A. Achim, P. Tsakalides and A. Bezarianos, “SAR image denoising via Bayesian wavelet shrinkage based on heavy -tailed modeling.,” *IEEE Transactions on Geoscience and Remote sensing.,* vol. 41, no. 8, pp. 1773-1784, Aug.2003.

[23] S. Solbo and T. Eltoft, “WMAP: A statistical specklefilter operating in the wavelet domain.,” *Int.J.Remote Sens.,* vol. 25, no. 5, pp. 1019-1036, Mar.2004.

[24] M. Bhuiyan, M. Ahmad and M. Swamy, “Spatially adaptive wavelet based method using the Cauchy prior for denoising the SAR images.,” *IEEE Transactions on Circuits and Systems for Video Technology.,* vol. 17, no. 4, pp. 500-507, Apr.2007.

[25] S. Solbo and T. Eltoft, “Homomorphic wavelet-based statistical despeckling of SAR images.,” *IEEE Transactions on Geoscience and Remote sensing.,* vol. 42, no. 4, pp. 711-721, Apr.2004.

[26] H. Xie, L. Pierce and F. Ulaby, “SAR speckle reduction using wavelet denoising and markov random field modeling.,” *IEEE Transactions on Geoscience and Remote Sensing.,* pp. 2196-2212, Oct.2002.

[27] M. C. Mihcak, I. Kozintsev, K. Ramchandran and P. Moulin, “Low complexity image denoising based on statistical modeling of wavelet coefficients.,” *IEEE Signal Processing Lett.,* vol. 6, pp. 300-303, Dec.1999.

[28] H. Xie, L. Pierce and F. Ulaby, “Despeckling SAR images using a low complexity wavelet denoising process.,” *in proceedings of IEEE International Geoscience and Remote Sensing Symposium.,* vol. 1, pp. 321-324, Nov.2002.

[29] F. Argenti, T. Bianchi and A. Alparone, “Multiresolution MAP despeckling of SAR images based on locally adaptive generalised Gaussian pdf modeling.,” *IEEE Transactions on Image Processing.,* vol. 15, no. 11, pp. 3385-3399, Nov.2006.

[30] F. Argenti., T. Bianchi. and A. Alparone., “Segmentation-based MAP despeckling of SAR images in the undecimated wavelet domain.,” *IEEE Transactions on Geoscience and Remote Sensing.,* vol. 46, no. 9, pp. 2728-2742, Sep.2008.

[31] H. Rabbani., M. Vafadust., P. Abolmaesumi. and S. Gazor., “Speckle noise reduction of medical ultrasound images in complex wavelet domain using mixturepriors.,” *IEEE Trans. Biomed.Eng.,* vol. 55, no. 9, pp. 2152-2160, Sep.2008.

[32] F. Argenti., T. Bianchi., A. Lapini. and L. Alparone., “Bayesian despeckling of SAR images based on Laplacian-Gaussian modeling of undecimated wavelet coefficients,” *in ICASSP 2011,* pp. 1445-1448, May 2011.

[33] J. J. Ranjani. and S. J. Thiruvengadam., “Dual tree complex wavelet transform based despeckling using interscale dependence,” *IEEE Trans.Geosci.Remote Sens.,* vol. 48, no. 6, pp. 2723-2731, Jun.2010.

[34] J. J. Ranjani. and S. J. Thiruvengadam., “Generalized SAR Despeckling Basedon DTCWT Exploiting Interscale and Intrascale Dependences.,” *IEEE Geoscience and Remote Sensing Letters.,* vol. 8, no. 3, May.2011.

[35] H. Biao, L. Honghau and J. Licheng, “The Despeckling of SAR Image Based Curvelet Transform.,” *Proceedings of APSAR 2009, 2nd Asian-Pacific Conference on Synthetic Aperture Radar.,* pp. 1080-1083, 2009.

[36] F. Argenti., T. Bianchi., G. M. di Scarfizzi. and L. Alparone., “LMMSE and MAP estimators for reduction of multiplicative noise in the non-subsampled contourlet domain.,” *Signal Process,* vol. 89, no. 10, pp. 1891-1901, Oct.2009.

[37] H. Biao, Z. Xiaohua, B. Xiaoming and F. Hongxiao, “SAR Image Despeckling Based on Non subsampled Shearlet Transform.,” *IEEE Journal of Selected Topics in Applied Earth Observations and Remote Sensing.,* vol. 5, no. 3, June 2012.

[38] W. G. Zhang, Q. Zhang and C. S. Yang, “Edge detection with multiscale products for SAR image despeckling,” *Electronic letters,* vol. 48, no. 4, Feb.2012.

[39] H. Zhong, J. Xu and L. Jiao, “Classification based nonlocal means despeckling for SAR image,” *in proc. of SPIE,* vol. 7495, Oct.2009.

[40] C. Deledalle, L. Denis and F. Tupin, “Iterative weighted maximum likelihood denoising with probabilistic patch-based weights,” *IEEE Transactions on Image Processing,* vol. 18, no. 12, pp. 2661-2672, Dec.2009.

[41] J. Polzehl and V. Spokoiny, “Propagation-separation approach for local likelihood estimation,” *Probability Theory and Related Fields,* vol. 135, no. 3, pp. 335-362, 2006.

[42] S. Parrilli, M. Poderico, C. V. Angelino and L. Verdoliva, “A nonlocal SAR image denoising algorithm based on LLMMSE wavelet shrinkage,” *IEEE Transactions on Geoscience and Remote Sensing,* vol. PP, pp. 1-11, 2011.

[43] L. Pennec, ,. E. and S. Mallat, “Bandlet Image Approximation And Compression,” *SIAM Journ of Multiscale Modeling and Simulation,* vol. 4, no. 3, pp. 992-1039, December 2005.

[44] E. Le Pennec and S. Mallat, “Sparse geometric image representations with bandlets,” *IEEE Transaction on Image Processing,* vol. 14, no. 4, pp. 423-438, April 2005.

[45] M. Jansen, M. Malfait and A. Bultheel, “Generalised cross validation for wavelet thresholding,” *Signal Process..,* vol. 56, no. 1, pp. 33-34, 1997.

[46] Y. Yu and S. T. Acton, “Specle reducing anisotropic diffusion,” *IEEE Trans. Image Process,* pp. 1260-1270, Nov.2002.

[47] K. He, J. Sun and X. Tang, “Guided image filtering,” *IEEE Trans. Pattern Anal.Mach. Intell..,* vol. 35, no. 6, pp. 1397-1409, Jun.2013.